An Interval-Based Metamodeling Approach to Simulate Material Handling in Semiconductor Wafer Fabs

Ola G. Batarseh, *Member, IEEE,* Dima Nazzal, and Yan Wang, *Member, IEEE*

***Abstract*—In this paper, we propose a new efficient metamodeling approach as a simulation platform to estimate the performance of automated material handling systems (AMHS) in a much shorter execution time. Our new mechanism is based on imprecise probabilities, in which the simulation model parameters are represented as intervals to incorporate unknown dependency relationships as total uncertainties. The interval-based metamodel provides reasonably accurate and fast estimates of the performance measures of interest. The performance measures from the interval-based simulation are represented as intervals that enclose the traditional real-valued simulation estimates. Using the SEMATECH virtual fab as a test bed, the metamodel of the wafer fab AMHS is implemented in JSim, a java-based discrete-event simulation environment, and the results are compared to the detailed large-scale simulation model to investigate the validity of the proposed approach.**

***Index Terms*—Automated material handling systems (AMHS), interval-based simulation (IBS), metamodel semiconductor manufacturing.**

I. Introduction

A. Semiconductor Manufacturing

Semiconductor technology, used in most modern electronics, is the building block of our information technology. The semiconductor industry is a vital contributor to the world economy, with $248.6 billion in sales worldwide in 2008, as reported by the Semiconductor Industry Association press-room [28]. The transition from 200 mm to 300 mm, and the potential transition to 450 mm wafer fabrication, is a key element of continuing productivity gains in semiconductor device manufacturing, and is driving fabs toward the full automation of material flow. AMHS are responsible for moving materials between production equipment and storage units to complete the processing of the wafers.

Constructing a 300 mm fab costs $2–3 billion [18], while a 450 mm fab is projected to cost $10 billion [21]. The AMHS represent 3–5% of the total fab cost [1]. For the AMHS to have acceptable return on investment and provide the expected support to the production equipment, efficient design and operational strategies must be investigated and tested in the design and redesign stages of the factory. An improperly designed or operated AMHS may introduce lot delays (increasing manufacturing cycle times) or cause tool idle time (reducing throughput or requiring excess capacity).

In recent years, particular attention has been given to the development of efficient design and operational strategies for wafer fabs. These efficient strategies must target increasing the throughput of the AMHS substantially with reduced delivery times. Further, the AMHS needs to be flexible and scalable to achieve the demands of the ever-changing semiconductor wafer fab.

Estimating AMHS performance in wafer fabs is difficult, because of the complexity of the systems. The International Technology Roadmap for Semiconductors [17] characterizes the AMHS as having several vehicles, operating on a network with loops, intersections, spurs, and shortcuts, serving many different pick-up/drop-off stations. The movement requests appear to be random, and although they exhibit some temporal correlations, these correlations are not strong enough to permit precise scheduling of the AMHS resources.

A typical 300 mm AMHS has a spine layout configuration, as illustrated in Fig. 1. Most wafer fabs use this bay layout [4], where each bay contains a group of similar process tools. A spine layout consists of a central material handling spine (interbay) and loops branching on both sides (intrabays) to serve production equipment (tools) in the bays. Automated storage units, referred to as stockers, are used to provide temporary buffering for work-in-process.

Almost all existing 300 mm AMHS are based on overhead hoist vehicles (OHV)—space-efficient vehicles traveling suspended on tracks above the main fab floor. The efficiency of an OHV-based AMHS is highly dependent on the vehicles' characteristics and control mechanism (i.e., speed, acceleration/deceleration, and dispatching rules). An AMHS with a small number of vehicles will cause long delays for lots waiting to be transported. Clearly, longer wait times imply longer delivery times. On the contrary, an excess of vehicles can cause traffic congestion in the interbay and intrabay systems because each of these units will frequently block other transporters that are traveling on the same path. As a

Manuscript received January 26, 2010; revised April 20, 2010 and June 21, 2010; accepted July 30, 2010. Date of publication August 16, 2010; date of current version November 3, 2010. This paper was recommended by Associate Editor S. P. Cunningham.

O. G. Batarseh and D. Nazzal are with the Department of Industrial Engineering and Management Systems, University of Central Florida, Orlando, FL 32816 USA (e-mail: obatarse@mail.ucf.edu; dnazzal@mail.ucf.edu).

Y. Wang is with the Department of Mechanical Engineering, Georgia Institute of Technology, Atlanta, GA 30332 USA (e-mail: yan.wang@me.gatech.edu).

Color versions of one or more of the figures in this paper are available online at http://ieeexplore.ieee.org.

Digital Object Identifier 10.1109/TSM.2010.2066993

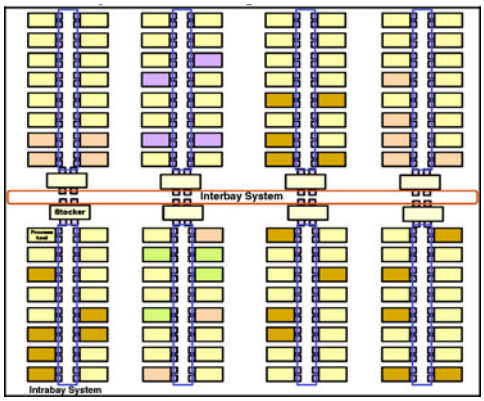

Fig. 1. AMHS in a spine layout: one interbay and eight intrabay systems (based on [16]).

result, delivery times increase significantly due to the longer delays that wafers experience while traveling in these highly congested systems.

Interaction between fab design (e.g., where to locate tools) and AMHS design (e.g., track configuration and fleet size) can have significant impacts on fab performance. Thus, the number of design alternatives for the AMHS is vast. Relying solely on discrete event simulation to navigate the AMHS design space means a commitment to a lengthy and expensive process, which may limit the range and number of alternatives that can be considered in the early stages of fab design. Simulation is ineffective as a decision support tool in the early phase of system design, where many configurations need to be considered. Our metamodeling approach, proposed and tested in this paper, is to simultaneously estimate accurate performance measures with shorter simulation time and incorporate input uncertainties in its estimations.

B. Motivation for Interval-Based Simulation (IBS)

Uncertainty and variability should be differentiated in simulation. Variability is due to the inherent randomness in the system. In the paper, variability is also referred to as stochastic uncertainty, simulation uncertainty, aleatory uncertainty, and irreducible uncertainty. Variability is irreducible even by additional measurements about the random variable of interest. The typical representation of variability is based on probability distributions. On the contrary, uncertainty is due to the lack of perfect knowledge or enough information about the system. Uncertainty is also known as epistemic uncertainty, reducible uncertainty, and model-form uncertainty. Since uncertainty is caused by lack of information about the system, it can be reduced by increasing our knowledge to fill the information gap. The *total uncertainty* in simulation consists of these two components, uncertainty and variability.

Input uncertainties in simulation have different sources, including lack of data, conflicting information, conflicting beliefs, lack of introspection, measurement errors and lack of information about dependency, and the difficulty to incorporate certain details of the real system due to limited modeling capabilities. In the AMHS, sources of uncertainties could be due to vehicle congestion and blocking, vehicles and equipment breakdowns, and insufficient sample data to estimate systems' random variables, such as interarrival and service times.

Recently, we proposed a new discrete-event simulation framework based on imprecise probabilities to model input uncertainties [2]. The parameters of the probability distributions in simulation are intervals; therefore, the associated probabilities become imprecise. Imprecise probabilities allow the total uncertainty in the simulation to be represented in a concise form. Interval-parameter statistical distributions are used to incorporate the two components in simulations. Consequently, interval-valued imprecise probabilities are used, and interval-random variates are generated for simulation.

The IBS is more reliable than traditional discrete-event simulation. A simulation mechanism is reliable if the *completeness* and *soundness* of its results with respect to uncertainties can be verified. A complete solution includes all possible occurrences. A sound solution does not include impossible occurrences. The proposed simulation mechanism enables us to obtain a *sound* and a *complete* solution by incorporating these uncertainty components in simulation.

The remainder of this paper is organized as follows. Section II presents a review summarizing past published papers relevant to our work. Section III introduces the interval-based metamodel. Section IV describes the implementation and validation of the IBS for the AMHS. Last, Section V concludes and briefly outlines our future work.

II. Literature Review

The objective of this paper is to use the IBS mechanism to model AMHS in wafer fabs. Herein, we introduce the background of our proposed simulation mechanism.

A. Input Uncertainty Quantification in Simulation

In our previous paper [2], we propose a new reliable discrete-event simulation based on intervals to model input uncertainties. Other related simulation techniques proposed to account for input uncertainties include second order Monte Carlo simulation [20], Bayesian approaches [7], [13], [36], [37], Delta method [5], [6], and bootstrapping [3]. In the Bayesian approaches, a prior distribution on each input parameter in the simulation is assigned to describe its initial uncertainty. The prior distribution is then updated to a posterior distribution based on the observed data. In the delta method, the total simulation output variance is estimated by two terms. The first term is the simulation variance, and the second one is the input parameter variance. In the bootstrap approach, the effect of input parameter uncertainty is quantified by percentile confidence intervals. Using the available information, the parameters are first estimated by the maximum likelihood estimation. The estimates are then used to draw new samples of the observations. See [15] for a detailed review and comparison.

B. Imprecise Probability

Imprecise probability is used in our proposed IBS. Imprecise probability uses a *set* of probabilities to quantify the uncertainty associated with an event. E, a pair of lower and upper probabilities $P(E) = \left[\underline{p}, \overline{p}\right]$ is used instead of a precise

value of $P(E) = p$ to represent the uncertainty. Imprecise probability captures the total uncertainty and represents its two components quantitatively. It provides a concise form to improve the robustness of simulation without the traditional sensitivity analysis operations.

Many representations of imprecise probabilities have been proposed. For example, the Dempster–Shafer evidence theory [8], [27] characterizes evidence with discrete probability masses associated with a power set of values, where belief–plausibility pairs are used to measure uncertainties. The behavioral imprecise probability theory [30] models uncertainties with the lower prevision (supremum acceptable buying price) and the upper prevision (infimum acceptable selling price) with behavioral interpretations. The possibility theory [9] represents uncertainties with necessity–possibility pairs. A random set [22] is a multivalued mapping from the probability space to the value space. Probability-bound analysis [10] captures uncertain information with p-boxes, which are pairs of lower and upper distribution functions. F-probability [34] incorporates intervals into probability values which maintain the Kolmogorov properties. Fuzzy probability [23] considers probability distributions with fuzzy parameters. A cloud [25] is a combination of fuzzy sets, intervals, and probability distributions. Recently, an imprecise probability with a generalized interval form [31], [33] was also proposed, where the probabilistic calculus structure is simplified based on the algebraic properties of the Kaucher arithmetic [19] for generalized intervals. IBS captures the total uncertainty using the generalized interval form.

C. Interval Analysis

1) *Interval Arithmetic:* IBS needs to compute and analyze interval data. Interval mathematics [24] is a generalization in which interval numbers replace real numbers, interval arithmetic replaces real arithmetic, and interval analysis replaces real analysis. Interval arithmetic was originally developed to solve the issue of numerical errors in digital computation due to the floating-point representation of numbers, where rounding and cancelation errors put the reliability of digital computation at risk. Intervals not only solve the problem of representation for real numbers on a digital scale but they also provide a generic form to represent uncertainties and errors in technical construction, measuring, computation, and range of fluctuation.

Interval arithmetic considers all possibilities of variation in worst cases in uncertainty propagation. Let $\left[\underline{x}, \bar{x}\right]$ and $\left[\underline{y}, \bar{y}\right]$ be two real intervals (i.e., $\underline{x}, \bar{x}, \underline{y}, \bar{y} \in R$) and $\circ$ be one of the four basic arithmetic operations for real numbers, $\circ \in \{+, -, \times, \div\}$. The set-based enclosure for intervals $\left[\underline{x}, \bar{x}\right]$ and $\left[\underline{y}, \bar{y}\right]$ is $\left[\underline{x}, \bar{x}\right] \circ \left[\underline{y}, \bar{y}\right] = \left\{x \circ y | x \in \left[\underline{x}, \bar{x}\right], y \in \left[\underline{y}, \bar{y}\right]\right\}$.

The corresponding interval arithmetic operations are defined for worst cases. For example $\left[\underline{x}, \bar{x}\right] + \left[\underline{y}, \bar{y}\right] = [\underline{x} + \underline{y}, \bar{x} + \bar{y}]$, $\left[\underline{x}\bar{x}\right] - \left[\underline{y}, \bar{y}\right] = \left[\underline{x} - \bar{y}, \bar{x} - \underline{y}\right]$ and $\left[\underline{x}, \bar{x}\right] \times \left[\underline{y}, \bar{y}\right] = \left[\min\left(\underline{x}\underline{y}, \underline{x}\bar{y}, \bar{x}\underline{y}, \bar{x}\bar{y}\right) \ \max\left(\underline{x}\underline{y}, \underline{x}\bar{y}, \bar{x}\underline{y}, \bar{x}\bar{y}\right)\right]$.

When the lower and upper bounds of an interval is equal, the point-wise interval is the same as a real number.

In the interval arithmetic, it is guaranteed that intervals calculated from the arithmetic include all possible combinations of real values within the respective input intervals, that is $\forall x \in \left[\underline{x}, \bar{x}\right], \forall y \in \left[\bar{y}, \bar{y}\right], \exists z \in \left[\underline{x}, \bar{x}\right] \circ \left[\underline{y}, \bar{y}\right], x \circ y = z$.

TABLE I
ILLUSTRATIONS OF THE SEMANTIC EXTENSION OF GENERALIZED INTERVAL

Algebraic Relation: $\left[\underline{x}, \bar{x}\right] + \left[\underline{y}, \bar{y}\right] = [z, \bar{z}]$	Corresponding Logic Interpretation
[2, 3] + [2, 4] = [4, 7]	$(\forall x \in [1, 3])(\forall y \in [2, 4])(\exists z \in [4, 7])(x + y = z)$
[2, 3] + [4, 2] = [6, 5]	$(\forall x \in [2, 3])(\forall z \in [5, 6])(\exists y \in [2, 4])(x + y = z)$
[3, 2] + [2, 4] = [5, 6]	$(\forall y \in [2, 4])(\forall x \in [2, 3])(\exists z \in [5, 6])(x + y = z)$
[3, 2] + [4, 2] = [7, 4]	$(\forall z \in [4, 7])(\forall x \in [2, 3])(\exists y \in [2, 4])(x + y = z)$

For example, $[1, 3] + [2, 4] = [3, 7]$ guarantees that $\forall x \in [1, 3], \forall y \in [2, 4], \exists z \in [3, 7], x + y = z$.

Similarly, $[3, 7] - [1, 3] = [0, 6]$ guarantees that $\forall x \in [3, 7], \forall y \in [1, 3], \exists z \in [0, 6], x - y = z$.

This is an important property that ensures the completeness of range estimations. When input variables are not independent, the output results will over-estimate the actual ranges. This affects only the soundness of estimations and not the completeness. Some special techniques have also been developed to avoid the range over estimations based on monotonicity properties of interval functions.

Generalized interval [12] is an extension of the above set-based classical interval with better algebraic and semantic properties based on the Kaucher arithmetic [19]. A generalized interval $\left[\underline{x}, \bar{x}\right]$ is not constrained by $\underline{x} \leq \bar{x}$ any more. Therefore, [4, 2] is also a valid interval and is called improper. The relationship between proper and improper intervals is established with the operator *dual*. Given a generalized interval $\left[\bar{x}, \underline{x}\right]$, *dual* $\left[\underline{x}, \bar{x}\right] = \left[\bar{x}, \underline{x}\right]$. The four examples in Table I illustrate the interpretations for operator "+," where the range estimation of $[\left[\underline{z}, \bar{z}\right] = [4, 7]$ in the first row is complete and the estimation of $\left[\underline{z}, \bar{z}\right] = [7, 4]$ in the fourth row is sound. $-, \times,$ have the similar semantic properties. The interpretation of the intervals varies according to its type (i.e., proper or improper) and its order in the interpreted algebraic relation. More information of generalized interval can be found in [31]–[33].

Based on the theorems of interpretability, the generalized interval provides more semantic power to help verify completeness and soundness of range estimations by logic interpretations.

2) *Interval Statistics:* The mean or average value of a set of random intervals $\left\{\left[\underline{x}_i, \bar{x}_i\right] | \underline{x}_i \leq \bar{x}_i, \underline{x}_i \in \mathrm{R}, \bar{x}_i \in \mathrm{R}\right\}$, where $i = 1, \ldots, N$, is also an interval. It should include the smallest possible and the largest possible means which can be calculated from any possible enclosed real number $x_i \varepsilon \left[\underline{x}_i, \bar{x}_i\right]$. Because the formula to calculate the mean is a monotone function, the lower bound of the interval mean is just the average of the left endpoints $\underline{x}_i$'s, and the upper bound is the average of the right endpoints $\bar{x}_i$'s [14]. Therefore, the *arithmetic mean* of random intervals is given by

$$[\mu, \bar{\mu}] = \left[\frac{1}{N}\sum_{i=1}^{N}\underline{x}_i, \frac{1}{N}\sum_{i=1}^{N}\bar{x}_i\right] \tag{1}$$

where N is the sample size of the random intervals.

Computing the range for the variance $[\underline{V}, \bar{V}]$, for a set of intervals, is an NP-hard problem. Several algorithms [11], [14], [35] were proposed to obtain the bounds on the variance. It was found that $\underline{V}$ can be computed in $0(N\log N)$ computational steps for N interval data samples. However, computing the upper bound of the variance $\bar{V}$ requires the computational effort that grows exponentially with the number of intervals in the data set. Only for several special cases, such as when intervals are not overlapped and there is no interval completely nested in another, $0(N\log N)$ and linear time algorithms are available to compute $\bar{V}$. In this paper, we represent data variation by the lower bound of interval data as

$$\sum_{i=1}^{N} \left(\underline{x}_i - \underline{\mu}\right)^2 / N - 1.$$

III. IBS

We proposed a new discrete-event simulation platform addressing the input uncertainties using intervals. The following is an introduction of the proposed mechanism that supports the interval metamodeling approach for AMHS.

A. IBS Modeling

Our new simulation mechanism incorporates input uncertainty factors by using intervals as input parameters. This allows us to simulate a range of scenarios from a set of probabilities, simultaneously. For instance, we represent the probability distribution of a random variable as $\exp\left([\underline{\lambda}, \bar{\lambda}]\right)$ instead of $\exp(\lambda)$. Our knowledge in the system, the level of uncertainty, is modeled as the width of the interval parameter, i.e., $[\bar{\lambda} - \underline{\lambda}]$. The larger the width is, the less knowledge we have about this parameter and vice versa. This representation of statistical distributions generates the lower and upper cumulative distribution functions, as illustrated in Fig. 2. As a result, the cumulative distribution function (*cdf*) associated with an input is no longer one crisp curve. Instead, we have a pair of *cdf*'s corresponding to the lower and upper bounds. Based on imprecise probabilities, a set of distributions can be enclosed within the bounds. Fig. 2 can be read in two equivalent ways; for a value of a random variable, the cumulative probability is represented by an interval probability $[\underline{F}(x), \bar{F}(x)]$. Conversely, for a cumulative probability $F(x)$, a corresponding random variate, $[\underline{x}, \bar{x}]$, can be generated, where $\underline{x}$ and $\bar{x}$ are the lower and upper bounds of the random interval variate, respectively.

Interval random variates instead of real-valued random variates are generated given a particular distribution. Consequently, the simulation proceeds using these random intervals. The generated random intervals include all possible random numbers which would be generated based on real-valued *cdf*'s that are enclosed by $[\underline{F}(x), \bar{F}(x)]$ with certain confidence level, continuous or discrete. For the purpose of this paper, we use the exponential distribution inverse transform method to generate interval interarrival times. For example, the lower and upper bounds of the random interval $[\underline{x}, \bar{x}]$, are generated by a pair of *cdf* curves with the parameters of $\bar{\lambda}$ and $\underline{\lambda}$, respectively, that is

$$\underline{x} = -\left(\frac{1}{\lambda}\right) \ln(1-u) \text{ and } \bar{x} = -\left(\frac{1}{-\underline{\lambda}}\right) \ln(1-u)$$

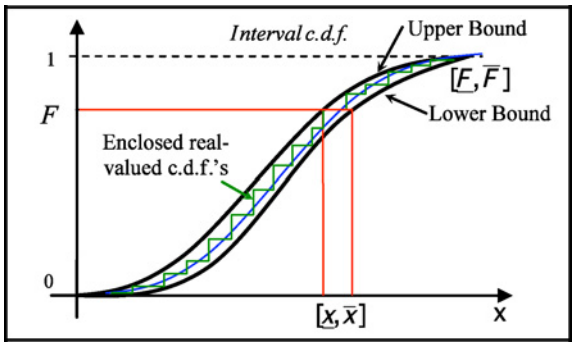

Fig. 2. Upper and lower cumulative distribution functions are used.

with a uniformly generated random number $u \in [0, 1]$. For distributions with multiple parameters, all combinations of the parameters need to be investigated. Then, the respective minimum and maximum from the combinations are selected as the lower and upper bounds of the generated interval random variate, for instance, for a normal distribution with the mean of $[\underline{\mu}, \bar{\mu}]$ and a standard deviation of $[\underline{\sigma}, \bar{\sigma}]$. The inverse transform method generates the interval random variate

$$[\underline{x}, \bar{x}] = [\min(c_1, c_2, c_3, c_4),\ \max(c_1, c_2, c_3, c_4)]$$

where $c_1 = F_r^{-1}(\underline{\mu}, \underline{\sigma})$, $c_2 = F_r^{-1}(\underline{\mu}, \bar{\sigma})$, $c_3 = F_r^{-1}(\bar{\mu}, \underline{\sigma})$, and $c_4 = F_r^{-1}(\bar{\mu}, \bar{\sigma})$ are real-valued random values generated individually from each parameter combination, where $F_r^{-1}(\mu, \sigma)$ is the inverse transform of the normal distribution with a mean μ and a standard deviation σ.

B. Interval Parameterization

An important question is how we select the probability distributions' interval parameters. If it is possible to collect data for an input random variate of interest, the set of data is used to fit a theoretical interval-based distribution form. First, the data is used to build a theoretical distribution with real-valued parameters as the traditional approach states. Based on the obtained distribution with real-valued parameters and the available data sample size, n the lower and the upper bounds of the interval parameters are estimated. The parameter bounds are calculated such that all possible real-valued scenarios are included in the simulation output with certain confidence level of $(1-\alpha)$ at any order $r = 1, 2, \ldots, n$.

This confidence is interpreted as the probability of having an assumed real-valued random variable x bounded by the corresponding random interval $[\underline{x}, \bar{x}]$ at any cumulative probability p in *cdf*. If the simulation is run from any real-valued parameter bounded by the interval parameter, the associated random variable at order r is given as x_r. This random variable is desired to be included within the interval $[\underline{x}_r, \bar{x}]$ with a certain level of confidence as follows:

$$P(x_r \in [x_r, \bar{x}_r]) \geq 1 - \alpha. \quad (2)$$

If the independence of the lower and upper bounds is assumed, the probability in (2) can be written as follows:

$$P(x_r \leq x_r \leq \bar{x}_r) = P(\underline{x}_r \leq x_r)(1 - P(\bar{x}_r \leq x_r)). \quad (3)$$

Order statistics is used to ensure that the probability in (3) at any order r is at least $(1-\alpha)$. If the real-valued variables are ordered as $x_{(1)}, x_{(2)}, \ldots, x_{(n)}$, the corresponding value of the cumulative probability p associated with the rth ordered observation is given by $(r-0.5)/n$. The sampling distribution of the transformed order statistics *cdf* is given by $G_r(x)$. $G_r(x)$ is interpreted as the probability that at least r observations in the sample do not exceed x and can be calculated [29] as follows:

$$G_r(x) = \sum_{j=r}^{n} \left[\binom{n}{j} (F(x))^j (1-F(x))^{n-j} \right] \tag{4}$$

where $F(x)$ is the *cdf* of any random variable. Based on the ordered statistics sampling distribution, the probability of having the rth random variable x_r between the rth bounds of the interval random variable $\left[\underline{x}_r, \bar{x}_r\right]$ is given by

$$P(\underline{x}_r \le x_r \le \bar{x}_r) = \underline{G}(x_r)(1-\bar{G}(x_r)) \tag{5}$$

where $\underline{G}(x_r)$ and $\bar{G}(x_r)$ are the upper and the lower sampling distribution, respectively. To find the lower parameter interval limit at any order r, we set the upper sampling distribution $\underline{G}(x_r)$ to $(1-\alpha)$ as follows:

$$\sum_{i=r}^{n} \left[\binom{n}{j} (\underline{F}(x_r))^j (1-\underline{F}(x_r))^{n-j} \right] \ge 1-a \tag{6}$$

where x_r is calculated from the inverse transform of the assumed distribution function with real-valued parameters as follows:

$$x_r = F^{-1}\left(\frac{r-0.5}{n}\right). \tag{7}$$

The probability in (5) can be used for any probabilistic distribution function by replacing the upper cumulative distribution function $\underline{F}(x)$ with the corresponding distribution form. In computing the lower interval parameter limit of $\underline{F}(x)$, a real value is first assumed. Then, it is decreased gradually until the desired probability of $(1-\alpha)$ is achieved.

On the contrary, for the upper interval parameter limit, we set the complement of the lower sampling distribution at any order r $\left(1-\bar{G}_r(x)\right)$ to $(1-\alpha)$ as follows:

$$\left(1 - \sum_{j=r}^{n} \left[\binom{n}{j} \left(\bar{F}(x_r)\right)^j \left(1-\bar{F}(x_r)\right)^{n-j} \right]\right) \ge 1-\alpha. \tag{8}$$

As well, the probability in (8) can be used for any probability distribution function by replacing the lower cumulative distribution function $\bar{F}(x)$ with the corresponding distribution form. Similarly, in computing the upper interval parameter of $\bar{F}(x)$, it is obtained by increasing its value until the probability of $(1-a)$ is achieved.

Here, we derive the specific form of (6) and (8) for the exponential distribution to demonstrate the use of the derived equations. Assume a stochastic process follows an exponential distribution with an estimated real-valued mean. An interval exponential distribution with the mean of $\left[\underline{\beta}, \bar{\beta}\right]$ is used to enclose the real-valued *cdf*, where $\beta \in \left[\underline{\beta}, \bar{\beta}\right]$. The upper bound *cdf* is associated with $\underline{\beta}$ and the lower bound *cdf* is with $\bar{\beta}$, substituting the exponential upper cumulative distribution function $\underline{F}(x_r) = 1 - e^{-x_{r/\underline{\beta}}}$ and the random variate as follows:

$$x_r = -\beta \ln\left(1 - \frac{r-0.5}{n}\right). \tag{9}$$

At order r in (6), we obtain the following:

$$P(\underline{x}_r \le x_r) = \sum_{j=r}^{n} \left[\begin{array}{l} \binom{n}{j} \left(1 - \left(1 - \frac{r-0.5}{n}\right)^{\beta/\underline{\beta}}\right)^j \\ \left(\left(1 - \frac{r-0.5}{n}\right)^{\beta/\underline{\beta}}\right)^{n-j} \end{array} \right]. \tag{10}$$

Substituting the exponential lower cumulative distribution function $\bar{F}(x) = 1 - e^{-x/\bar{\beta}}$ and the random variate x_r in (9) at order r in (8), we get the following:

$$P(\underline{x}_r \le \bar{x}_r) = 1 - \sum_{j=r}^{n} \left[\begin{array}{l} \binom{n}{j} \left(1 - \left(1 - \frac{r-0.5}{n}\right)^{\beta/\underline{\beta}}\right)^j \\ \left(\left(1 - \frac{r-0.5}{n}\right)^{\beta/\bar{\beta}}\right)^{n-j} \end{array} \right]. \tag{11}$$

We calculate the lower interval mean $\underline{\beta}$ at any order r as follows. First, we set $\underline{\beta} = \beta$. Given a particular value of β and the available sample size n, we start gradually reducing the value of $\underline{\beta}$ and compute the probability of enclosure using (10) repeatedly until it reaches the predetermined probability of $(1-\alpha)$. The resulted $\underline{\beta}$ is the value satisfying the desired probability at the predetermined order r. Similarly, we use (11) to find $\bar{\beta}$ for the desired probability of enclosure by gradually increasing the initial value of $\bar{\beta} = \beta$. Since the parameter is sensitive up to three significant digits, 0.001 is used as the incremental step size.

The factors that decide the lower and the upper bounds of the interval parameters include: 1) sample size n; 2) the desired confidence of enclosure $(1-\alpha)$; and 3) the order r. First, as n increases, the parameters' bounds get narrower. This is because the uncertainty related to the random variable decreases by increasing the sample size. Second, as the desired degree of enclosure $(1-\alpha)$ increases, the bounds have to be wider to enclose all possible real-point parameters. For a desired enclosure of $(1-\alpha)$, we notice that the ratio of $\bar{\beta}/\beta$ obtained is the same for a particular order r and a sample size of n. This also applies to the ratio of $\underline{\beta}/\beta$. Given n = 100 and $\alpha = 0.1$, Fig. 3(a) and (b) depicts the ratio of $\underline{\beta}/\beta$ and $\bar{\beta}/\beta$ with the orders $r = 1, 2 \ldots 1000$, respectively.

Due to the narrow width of the *cdf* bounds, i.e., the *cdf* curves become flatter at those bounds, it becomes more difficult to bound the real-valued variable at small and very large orders. If we use the interval parameter obtained at these orders, we are estimating a complete solution that includes all possible occurrences at all orders. For instance, the lower mean at these orders has the minimum value, and on the contrary, the upper mean has the maximum value. The ratios for the lower and the upper parameters to the real-valued mean are approximately the same for middle orders. The simulation analyst can choose the interval-parameter associated with any order r based on the desired level of including all possible solutions. If a complete solution is desired, the analyst uses the smallest order, $r = 1$ to include all possible mean values of all orders. The associated mean at order $r = 1$ is the smallest and the largest possible parameter value for the lower

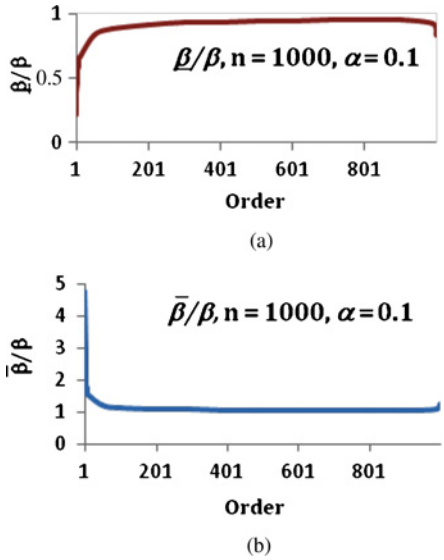

Fig. 3. (a) Ratio of $\underline{\beta}/\beta$ with order r. (b) Ratio of $\bar{\beta}/\beta$ with order r.

and the upper bounds, respectively. According to the desired level of enclosure to the possible solutions, each simulation analyst then select a certain order r. In this paper, we use order $r = 100$ with a confidence level of $\alpha = 0.1$ to estimate the interval-parameters needed in simulation.

IV. AMHS Metamodel

The AMHS metamodel is an abstraction of the detailed simulation model. In our implementation, we represent the exact process routes by a number of move requests and their routing probability obtained from the detailed simulation.

A. System Description

The general layout of the example used to represent the AMHS is composed of 24 machines: 48 stations (24 loading and 24 unloading stations). This layout is based on a 300 mm virtual semiconductor fabrication facility developed and published by International SEMATECH [26]. The vehicles travel on a unidirectional closed-loop at a constant speed of 3 f/s. The product family modeled is SEMATECH's 300 mm aluminum process flow for 180 nm technology. Such technology node contains 6 metal layers and 21 masks. For this single product family, ten products are continuously released into the process. The release rate is 20 000 wafers per month (wpm). The processing route consists of approximately 316 operations (i.e., steps). In addition, there are 60 different workstations and about 300 tools. Wafers travel in carriers (lots) that hold 25 units. The 300 mm Wafer Fab Model has 24 bays arranged using a spine layout configuration similar to the layout previously shown in Fig. 1. We will only model the central aisle, also referred to as the interbay AMHS that transfers the wafers between the 24 bays. A schematic of the interbay system is shown in Fig. 4.

The software used for detailed simulation is AutoMod 11.1. In order to obtain steady-state estimates, we start with an empty system and warm it up until it reaches steady state as indicated by the steady level of work-in-process in the system.

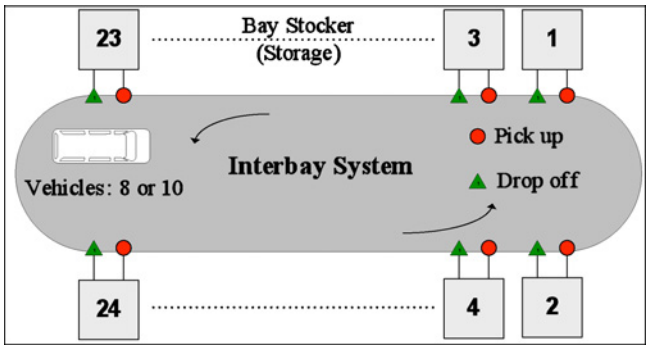

Fig. 4. Schematic of the modeled interbay system.

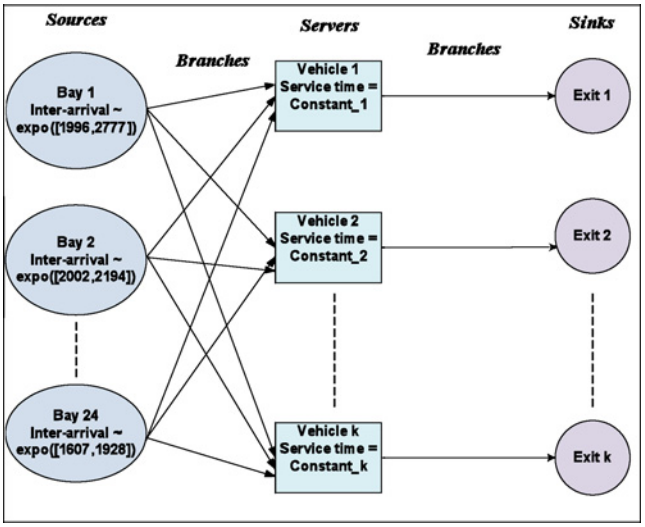

Fig. 5. Object-oriented modeling for AMHS implemented in JSim.

After the warm-up period, all the appropriate statistics are collected. We refer to the results obtained from this simulation as "detailed results" because this simulation model explicitly models the wafers movement between the different bays, and these are assumed to be accurate estimates.

B. Interval-Based Metamodel

The metamodel is implemented in a java-based object-oriented simulation package, *JSim*. *JSim* is considered the basic platform to execute the IBS. Any extension to new objects can be built and added to the package. Object-oriented languages, like Java, are flexible to allow for customized models of different applications. In *JSim,* we use *Source* to represent the bays that generate the *Entities (group of wafers, also referred to as lots)* with given interarrival times. *Server* is used to characterize the vehicles that transfer *Entities* in the interbay system. Finally, exits in the system are represented using a *Sink* to dispose an entity upon the end of its service time. Fig. 5 illustrates the object-oriented modeling for the AMHS in *JSim.*

Essentially, the metamodel does not explicitly model the wafers' flow through each bay in its process route. Instead, details concerning the processing of wafers are implicitly represented by the number of move requests received by the AMHS. These moves are summarized in the metamodel as

"From-To" matrices, which describe the rate of moves between two different bays of the fab. The From-To matrices are generated from the production volume and the process route of the products in SEMATECH's model. The basic unit in the metamodel is the vehicle that is dedicated to one move request, and each move request is considered a single lot that represents a group of 25 wafers. Our metamodel does not study what happens to a move request after it gets delivered to its destination. The from-to matrix represents the frequency of moves between each two bays, which was created from the product recipe (route) in the detailed simulation. The metamodel results are referred to as "IBS Metamodel Results." In this paper, we implemented two dispatching rules. oldest load closest vehicle (OLCV) and closest load closest vehicle (CLCV). The two dispatching rules are implemented in two models to incorporate the differences in deciding the priorities for processing wafer fabs using the two rules.

C. Interval Input Random Variates

In this AMHS system, it is assumed that we do not have enough information to be certain about the parameters of the interarrival times for the bays. Only 1000 sample-points from the "detailed simulation" are collected to fit an exponential distribution with real-valued parameter β using the maximum likelihood estimator (MLE) for each bay. Based on the value obtained from the MLE, the proposed interval-parameterization technique in Section III-B is used to find the interval mean of the exponential distribution for the interarrival times at order $r = 100$ with $\alpha = 0.1$. The obtained ratios of $\frac{\beta}{\underline{\beta}}$ and $\frac{\bar{\beta}}{\beta}$ are 0.8506 and 1.1831, respectively. Hence, we multiply these ratios by the real-valued mean obtained from the MLE for each bay to find the interval mean. For example, the real-valued average interarrival time obtained for the first bay is $\beta = 2347.40$ s. Hence, the corresponding interval mean at $r = 100$ is $\left[\underline{\beta}, \bar{\beta}\right] = [0.8506\beta,\ 1.1831\beta] = [1996.70, 2777.21]$. The interarrival times of entities of the 24 bays with the real-valued parameters and the associated intervals are available upon request. Because order $r = 100$ is selected out of $n = 1000$, at least 90% enclosure of the ordered real-valued random variates between their corresponding interval variates is guaranteed. Moreover, a probability of at least $(1-\alpha) = 90\%$ is guaranteed to enclose the real-valued variate between the bounds of interval variate at each order. For instance, if we run these bounds n times, we are confident that at least $n(1-\alpha)$ times the interval variates enclose the real variates generated from the exponential distribution $\exp(\beta)$.

The obtained intervals for the interarrival times in Table II are used to run the metamodel to enclose the detailed simulation results. Note that no entities are generated from bays 6 and 23. Bays 6 and 23 have no flows based on the SEMATECH model. Additionally, travel times of vehicles are assumed to be constant. The routing probabilities matrix and the vehicles' from-to travel times matrix used to generate our results are available upon request.

D. Metamodel Simulation Process

As mentioned previously, we study two dispatching rules to serve the entities for this metamodel: 1) OLCV, and 2) CLCV.

TABLE II
INTERARRIVAL TIMES REAL-POINT EXPONENTIAL MEANS AND INTERVALS (S)

Bay	Real-point Mean (s)	Interval Mean (s)
1	2347.40	[1996.70, 2777.21]
2	2002.39	[1703.23, 2369.03]
3	1164.78	[990.76, 1378.05]
4	1270.86	[1080.99, 1503.55]
5	1170.68	[995.78, 1385.03]
6	0	[0, 0]
7	2345.79	[1995.33, 2775.31]
8	303.92	[258.51, 359.56]
9	3496.66	[2974.26, 4136.89]
10	563.48	[479.29, 666.65]
11	881.46	[749.77, 1042.85]
12	1280.50	[1089.19, 1514.96]
13	1407.37	[1197.11, 1665.06]
14	1401.75	[1192.33, 1658.42]
15	1396.91	[1188.21, 1652.69]
16	2332.05	[1983.64, 2759.05]
17	2331.11	[1982.84, 2757.94]
18	2791.37	[2374.34, 3302.47]
19	4675.92	[3977.33, 5532.08]
20	7061.44	[6006.46, 8354.39]
21	1993.41	[1695.60, 2358.41]
22	2327.75	[1979.98, 2753.96]
23	0	[0, 0]
24	1759.17	[1496.35, 2081.28]

The OLCV dispatching rule ensures that waiting entities are served based on a first-in-first-out principle while selecting the closest idle vehicle to serve the entities. Similarly, the CLCV dispatching rule selects the closest vehicle to serve an entity. However, it serves the closest waiting entity when a vehicle becomes idle. The two scenarios are simulated in this paper varying the fleet size between 8 and 10 vehicles.

In IBS, entities are generated with interval arrival times, i.e., $\left[\underline{a}_i, \bar{a}_i\right]$ for entity i. An important question here is which entity to serve first when the interval arrival times of the entities overlap. We decide the sequence of serving entities based on the upper bounds of their interval arrival times $\bar{a}_i$, i.e., the latest time the entities arrive at the system. Therefore, the entities arrive at time $\left[\underline{a}_i, \bar{a}_i\right]$ and leave the system at a departure time given as $\left[\underline{d}_i, \bar{d}_i\right]$ for entity i

$$\left[\underline{d}_i, \bar{d}_i\right] = \left[\underline{sst}_i, \overline{sst}\right] + \left[\underline{s}_i, \bar{s}_i\right] \tag{12}$$

and $\left[\underline{s}_i, \bar{s}_i\right]$ is the interval service time to transfer entity between the bays including the loading time. The interval service time is considered as a point-wise interval, i.e., $\underline{s}_i, \bar{s}_i$, because service times are assumed to be constant. Following a predetermined dispatching rule, the interval service start time for entity i, denoted as $\left[\underline{sst}_i, \overline{sst}_i\right]$ is determined by

$$\left[\underline{sst}_i, \overline{sst}_i\right] = [\max(\underline{a}_i, \underline{d}_{i-1}),\ \max(\bar{a}_i, \bar{d}_{i-1})]. \tag{13}$$

From the IBS metamodel, we are interested in calculating the interval response time to move requests. The response time to a move request, i.e., the waiting time in the queue, is the sum of the waiting time until a vehicle becomes idle and the travel time of empty vehicle to the load location. In addition,

we study the enclosure of these intervals to the real-valued response time to move requests obtained from the detailed simulation. The interval response time to move requests is now calculated as follows:

$$\left[\underline{w_i}, \overline{w_i}\right] = \left[\underline{sst_i}, \overline{sst_i}\right] - dual\left[\underline{a_i}, \bar{a}_i\right]. \tag{14}$$

Equation (14) gives a range estimate to the waiting time of the entities to be served. The *dual* operator is used to estimate a sound solution to the response time to move requests in comparison with the complete solution that results from the interval arithmetic to estimate best-case and worst-case scenarios. The solution provided by (14) is a sound solution that does not include impossible solutions. Hence, some real-valued solutions may be out of the calculated bounds from (14). But they all are bounded by the complete solution from the following:

$$\left[\underline{w_i}, \overline{w_i}\right] = \left[\underline{sst_i}, \overline{sst_i}\right] - \left[\underline{a_i}, \bar{a}_i\right]. \tag{15}$$

However, the complete solution usually overestimates and gives every wide bounds. In this IBS metamodel, we use (14) for calculations. Assume that entity interval arrival time is given as [12.34, 17.64] s and the interval service start time is given as [18.45, 25.65] s. If (14) is used to estimate the interval response time, the solution is [6.11, 8.01] s and its interpretation is as follows:

$$\begin{aligned}&(\forall a_i \in [12.34, 17.64])(\forall w_{\downarrow} i \in [6.11, 8.01]])\\ &(\exists sst_i \in [18.45, 25.65])(sst_i - dual(a_i) = w_i).\end{aligned} \tag{16}$$

However, if (15) is used to calculate the interval response time, the complete solution is [0.81, 13.31] s and interpreted as follows:

$$\begin{aligned}&(\forall a_i \in [12.34, 17.64])(\forall sst_i \in [18.45, 25.65])\\ &(\exists\, w_i \in [0.81, 13.31])(sst_i - a_i = w_i).\end{aligned} \tag{17}$$

Moreover, we represent the variation in the interval response time obtained from the IBS by calculating the standard deviations for the lower bounds $\underline{w_i}$'s.

In addition, the vehicles' utilization is measured by the percentage of time the vehicle is loaded, travels with entities, and unloaded. In the IBS metamodel, the vehicles' average utilizations are given as real-valued estimates. The average utilization are calculated as the percentage of time the vehicles travel to serve an entity, regardless of whether the entity arrives at its lower bound $\underline{a_i}$, or its upper bound $\bar{a}_i$.

Such models are valuable to early stages of design because it allows the designer to experiment with different design strategies for the number of vehicles and the flow path layout. Increasing the number of vehicles has the potential to reduce the expected response time to move requests, which is directly related to the production cycle time of the wafers. Reducing the production cycle time is always a priority for fabs because of the short life span of these types of products. However, there is an optimal number of vehicles to install, beyond which the improvement in response time is marginal and may not be justifiable financially. Fab designers benefit from the metamodel as it provides fast answers to different design scenarios. The importance of monitoring the standard deviation of response

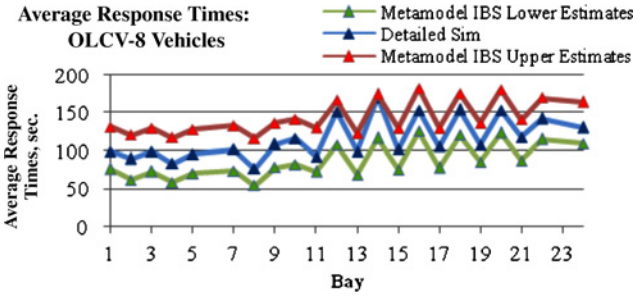

Fig. 6. Average response times to move requests for OLCV: eight vehicles.

times is twofold: first, inconsistent response times translate to inconsistent delivery times to the end customer, an undesirable and expensive situation as increased variability is directly related to increased levels of safety stocks. Second, from simple queueing formulas, we know that increased variability propagates through a manufacturing line and increases the work-in-process and the queueing delays at subsequent stages.

E. Comparison of the Metamodel Results to the Detailed Simulation Output

In the *JSim* implementation of the IBS metamodel, we executed $n = 5$ independent replications for both OLCV and CLCV scenarios. The number of replications was selected so that the confidence intervals of the simulation outputs have a half-width to mean ratio of less than 5%. Each replication has a length of m = 200 days. Conservatively, we chose a warm-up period of l = 100 days to reach the steady-state. This section summarizes the simulation results. The performance measures include the interval time to move request $\left[\underline{w_i}, \bar{w}_i\right]$, the standard deviation of the lower bounds $s(\underline{w_i})$, and the average utilization of the vehicles ρ, with respect to the two dispatching rules.

1) *Oldest Load Closest Vehicle Rule:* First, we present the results obtained from the OLCV dispatching rule with the simulation of eight and ten vehicles to transfer entities. The simulation results of the average response time using eight vehicles are shown in Fig. 6. We compare the lower and upper bounds obtained from the IBS with the detailed simulation results obtained from AutoMod.

The lower and the upper estimates of the interval results enclose the detailed simulation results. Thus, the uncertainties associated with the interarrival times of the entities at the bays are incorporated. For instance, we report the response time for bay 1 as [76.35, 131.33] s as opposed to the detailed real-valued simulations that only give an estimate of 81.64 s. The interval estimations of the performance measures are considered more reliable as it provides a range of solutions that enclose the detailed simulation results incorporating uncertainties in the interarrival times. The gap between the interval bounds and the detailed simulation results is due to modeling the uncertainty component in simulation, which is expected and desired. From the results, we notice that the differences between the bounds and the detailed simulation results are consistent for the different bays in the system.

One might ask how these intervals differ from the standard confidence intervals. We answer this concern by referring to these traditional methods as statistical measures that incorporate only the variability component in their estimates. For

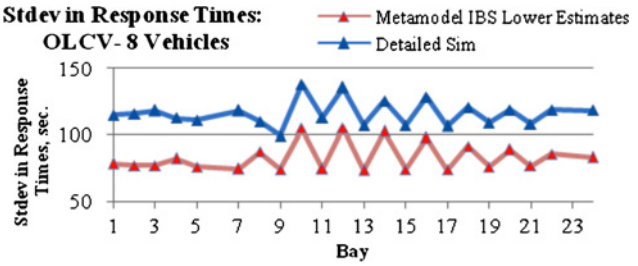

Fig. 7. Standard deviation of response time to move requests for OLCV: eight vehicles.

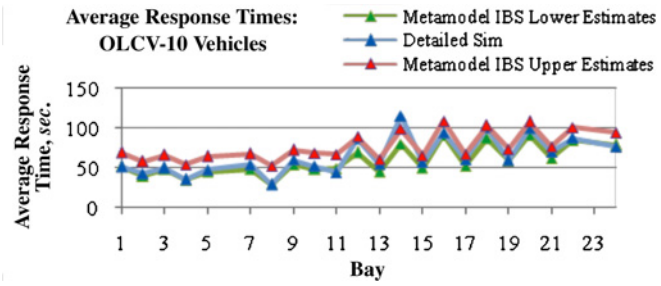

Fig. 8. Response time to move requests for OLCV: ten vehicles.

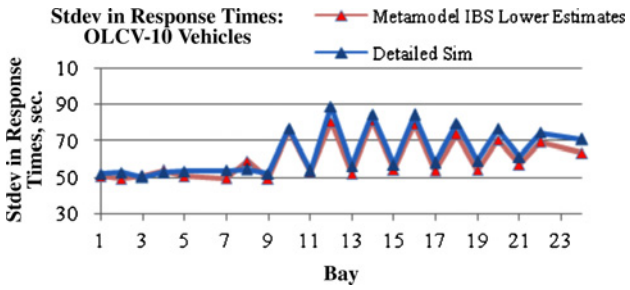

Fig. 9. Standard deviation in response time to move requests for OLCV: ten vehicles.

instance, the traditional confidence interval limits represent a lower and upper bounds of the estimates based on a marginal error in the readings with a certain level of confidence. The interval limits are calculated as the mean value of the outputs of multiple simulation runs +/- a quantity that represents the standard deviation in these outputs. The standard deviation is attained within these readings because of the different random number streams used in the simulation runs. Given that all simulation runs use a fixed value of the parameters, the interpretation of this interval is that the average mean of the performance measure is included between these interval limits with a certain level of confidence. They do not represent the uncertainty in their bounds. However, our interval estimates incorporate the variability and the uncertainty components explicitly in each single simulation run. The input distributions with imprecise parameters provide interval estimates to the performance measures of interest from each simulation run. Because the uncertainty is propagated in the simulation runs, our intervals are not a result of running multiple simulation runs. Instead, they are obtained from running the IBS with imprecise parameters where uncertainty is incorporated within one single run. In addition, in traditional simulation output analysis, confidence intervals are indicators of the confounded effect of variability and uncertainty. In IBS, the effects of the two components are quantified separately and can be treated in different ways in decision making. Therefore, the IBS intervals results are considered more reliable than the traditional confidence intervals.

Furthermore, the standard deviations of the lower bound response times are collected and compared with those from the detailed simulation. Fig. 7 depicts the difference in the standard deviations for the detailed and IBS metamodel with eight vehicles. The standard deviations from the detailed simulation are larger than the ones obtained from the IBS metamodel. However, they both follow the same pattern for different bays. The lower standard deviation of the IBS metamodel is less than that from the detailed simulation model because it is calculated from the lower response times. Because of the equal values of mean and standard deviation in an exponential distribution, the lower response times resulted from the simulation of entities arriving at the system have a lower variability.

In addition, the average utilization of the eight vehicles is reported as 56.66% for the detailed simulation, and 48.70% for the IBS metamodel. The difference is due to that the vehicle traveling times in the IBS metamodel are averages of the actual ones in the detailed model without variations.

Fig. 8 presents the response times to move requests with ten vehicles. In this setting, the system becomes more saturated with more vehicles and the response time decreases as the availability of the vehicles increases. The increase in availability of the vehicles reduces the uncertainty in the response times to move requests. In other words, the response times to move requests in such scenarios are less uncertain because there are more vehicles to serve the entities whether they arrive at their lower or upper arrival times. Therefore, the differences between the response times from the detailed simulation and the lower or upper bounds from the metamodel are small. The response times of the detailed simulation for all bays except bays 1, 8, 11, 14, and 24 are enclosed by the corresponding intervals from the IBS metamodel. When order $r = 100$ was selected, we were aiming a 10% of enclosure for each bay separately not for all the bays together. This is interpreted as follows: the intervals means at each bay includes at least 90% of real-point means obtained from traditional simulation. Again, the lack of complete enclosure using ten vehicles in simulation is because the system is more saturated with vehicles than it is needed.

The standard deviations associated with the response times using ten vehicles are illustrated in Fig. 9. The standard deviations for response times in the detailed simulations are slightly greater than the standard deviations of lower bounds from the IBS metamodel. Again, both estimates follow the same pattern. The utilization of the ten vehicles from the detailed simulation is given as 43.38% down to 39.94% for IBS metamodel.

2) *Closest-Load Closest-Vehicle Rule:* We also model the AMHS using the CLCV dispatching rule for eight and ten vehicles. Fig. 10 presents the average response times for eight vehicles and the standard deviation of the response times for each bay. The average response times obtained from the

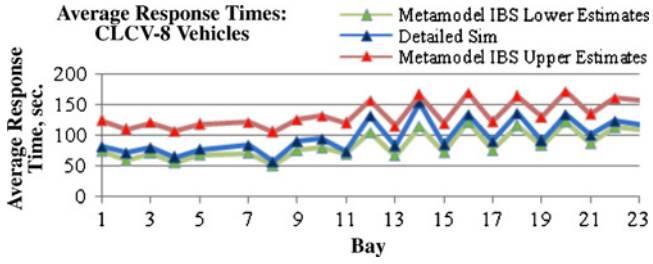

Fig. 10. Response time to move requests for CLCV: eight vehicles.

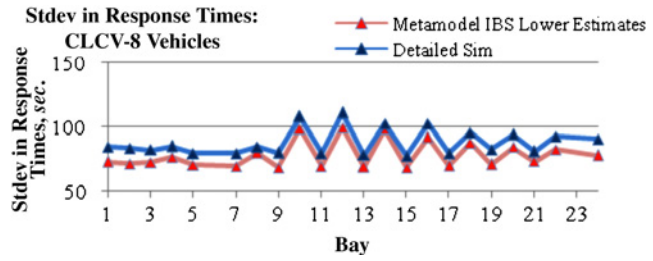

Fig. 11. Standard deviation in response time to move requests for CLCV: eight vehicles.

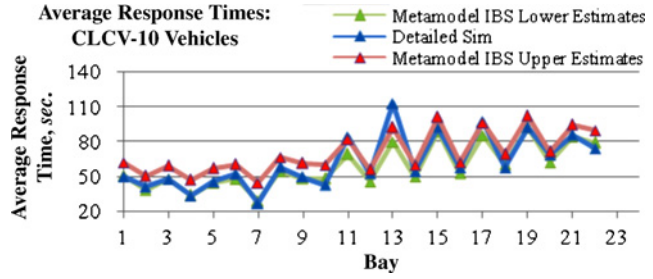

Fig. 12. Response time to move requests for CLCV: ten vehicles.

detailed simulation are well-enclosed between the lower and the upper bounds obtained from the IBS metamodel.

Fig. 11 compares the standard deviations of the lower bounds from the metamodel and the ones from the detailed simulation. The average utilization of the vehicles for this scenario is reported as 54.60% for the detailed simulation and as 48.26% for the IBS metamodel.

As for ten vehicles, the simulation results are summarized in Figs. 12 and 13. The average response times obtained from the detailed simulation model are not well enclosed within the bounds of IBS metamodel. As mentioned above, the reason is due to the increased number of vehicles. Hence, the average response time is comprised mostly of travel times of empty vehicles to the waiting entities. Vehicles are mostly available when a request is issued. In addition, the standard deviations of the two simulations are quite close to each other with at most 16.28% of relative differences. The average utilizations of vehicles are 41.47% for the detailed simulation and 35.62% for IBS metamodel. There is no relationship noticed between the selected dispatching rule and the enclosure of the IBS results to the detailed simulations outputs. The enclosure of the IBS to the detailed simulation is shown for most of the bays regardless of the dispatching rule.

In summary, the IBS metamodel offers interval estimations for average response times enclosing the detailed simulations

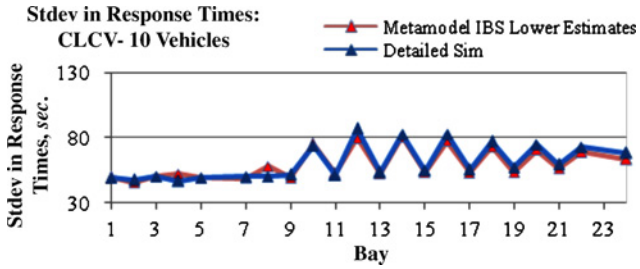

Fig. 13. Standard deviation in response time to move requests for CLCV: ten vehicles.

with certain level of confidence. Moreover, the interval estimations model input uncertainties in the interarrival times of entities. The input uncertainties come from unknown dependency between bays, machine breakdown, and vehicle congestion. The standard deviations obtained from lower bounds follow the same pattern as the detailed simulation variations. However, the IBS standard deviations are less than the corresponding results obtained from the detailed simulations. The vehicles' utilizations calculated from IBS are also smaller than the detailed simulation estimates.

The simulation time based on the metamodel is significantly reduced. On a dual-processor workstation, one run of the IBS model takes less than 2 min, whereas the detailed simulation requires 30 min on average.

V. Conclusion

In this paper, we proposed an AMHS metamodel to simulate a 300 mm wafer fab. It was based on a new interval-based discrete-event simulation. The parameters of probability distributions for the interarrival times in the simulation are intervals instead of traditional precise numbers. We implemented the metamodel in a java-based object-oriented simulation package. The obtained interval estimates to the mean response time are considered more reliable compared to the real-valued estimates, since they incorporate the total uncertainty in simulation. The IBS enables logical interpretation of its solutions where the completeness and soundness of the results can be verified with respect to uncertainty. More research is needed to quantify the enclosure probability of the complete and sound solutions obtained from the IBS.

Experimental comparisons indicated that the IBS metamodel performs very well for estimating the average and standard deviation of response times at each bay. They are critical performance measures when evaluating the AMHS. Our numerical results also showed that the metamodel enclosure of the detailed simulation results deteriorates as the servers (vehicles in this case) are under-utilized. This is expected because as the AMHS becomes less congested, uncertainty in its performance reduces and the advantage of interval performance measures becomes less obvious.

It has been noted earlier that the significance of the metamodel is the simplification of simulation models but still incorporating the effects of uncertain factors, such as vehicle congestion and blocking, and vehicles and equipment breakdowns. There is also substantial room for improvement in our metamodel. For example, we can model the specifics of the

path layout design in order to allow for its uncertainties propagation through our model and obtain more reliable results.

Further research is needed to study the dispersion associated with the interval data obtained from the IBS. Currently, we use the standard deviation of lower bounds to measure the dispersion of intervals. New interval-based statistics will be more reliable. More investigation of the logical interpretations from the interval results is also needed. This can help us to understand more simulation details thus support robust decision making in layout selection.

REFERENCES

[1] T. Arzt and F. Bulcke, "A new low cost approach in 200 mm and 300 mm AMHS," Semiconductor Fabtech, 1999 [Online]. Available: http://www.fabtech.org

[2] O. G. Batarseh and Y. Wang, "Reliable simulation with input uncertainties using an interval-based approach," in *Proc. Winter Simulation Conf.*, 2008, pp. 344–352.

[3] R. Barton and L. Schruben, "Resampling methods for input modeling," in *Proc. Winter Simulation Conf.*, 2001, pp. 372–378.

[4] G. Cardarelli and P. J. Pelagagge, "Simulation tool for design and management optimization of automated interbay material handling and storage systems for large wafer fab," *IEEE Trans. Semiconduct. Manufactur.*, vol. 8, no. 1, pp. 44–49, Feb. 1995.

[5] R. C. H. Cheng and W. Holland, "Sensitivity of computer simulation experiments to errors in input data," *Statist. Computat. Simulation*, vol. 57, pp. 219–241, 1997.

[6] R. C. H. Cheng and W. Holland, "Two-point methods for assessing variability in simulation output," *Statist. Computat. Simulation*, vol. 60, pp. 183–205, 1998.

[7] S. E. Chick, "Bayesian analysis for simulation input and output," in *Proc. Winter Simulation Conf.*, 1997, pp. 253–260.

[8] A. Dempster, "Upper and lower probabilities induced by a multi-valued mapping," *Ann. Math. Statist.*, vol. 38, no. 2, pp. 325–339, 1967.

[9] D. Dubois and H. Prade, *Possibility Theory: An Approach to Computerized Processing of Uncertainty*. New York: Plenum, 1988.

[10] S. Ferson, V. Kreinovich, L. Ginzburg, D. S. Myers, and K. Sentz, "Constructing probability boxes and Dempster-Shafer structures," Sandia Nat. Lab., Albuquerque, NM, Tech. Rep. SAND2002-4015, 2002.

[11] S. Ferson, V. Kreinovich, J. Hajagos, W. Oberkampf, and L. Ginzburg, "Experimental uncertainty estimation and statistics for data having interval uncertainty," Sandia Nat. Lab., Albuquerque, NM, Tech. Rep. SAND2007-0939, 2007.

[12] E. Gardenes, M. A. Sainz, L. Jorba, R. Calm, R. Estela, H. Mielgo, and A. Trepat, "Modal intervals," *Reliable Comput.*, vol. 7, no. 2, pp. 77–111, 2001.

[13] P. Glynn, "Problems in Bayesian analysis of stochastic simulation," in *Proc. Winter Simulation Conf.*, 1986, pp. 376–383.

[14] L. Granvilliers, V. Kreinovich, and N. Müller, "Novel approaches to numerical software with result verification," in *Numerical Software with Result Verification*, LNCS 2004, vol. 2991. pp. 274–305, 2003.

[15] S. Henderson, "Input model uncertainty: Why do we care and what should we do about it?" in *Proc. Winter Simulation Conf.*, 2003, pp. 90–100.

[16] ITRS. (2005). *Factory Integration Chapter Material Handling Backup Section* [Online]. Available: http://public.itrs.net/reports.html

[17] ITRS. (2005). *Factory Integration* [Online]. Available: http://www.itrs.net

[18] S. Jones, "300 mm perceptions and realities," *Semiconduct. Int.*, vol. 26, pp. 69–72, 2003.

[19] E. Kaucher, "Interval analysis in the extended interval space IR," *Comput. Suppl.*, vol. 2, pp. 33–49, 1980.

[20] H. Lan, B. L. Nelson, and J. Staum, "A confidence interval for tail conditional expectation via two-level simulation," in *Proc. Winter Simulation Conf.*, 2007, pp. 949–957.

[21] M. LaPedus. (2008). "450-mm fabs to run $10B; scaling to slow," *IEDM* [Online]. Available: http://www.eetimes.com

[22] I. Molchanov, *Theory of Random Sets*. London, U.K.: Springer, 2005.

[23] B. Möller and M. Beer, "Fuzzy randomness," in *Uncertainty in Civil Engineering and Computational Mechanics*. Berlin, Germany: Springer, 2004.

[24] R. E. Moore, *Interval Analysis*. Englewood Cliffs, NJ: Prentice-Hall, 1966.

[25] A. Neumaier, "Clouds, fuzzy sets, and probability intervals," *Reliable Comput.*, vol. 10, no. 4, pp. 249–272, 2004.

[26] SEMATECH. (2001). *Fab Simulation Modeling Software* [Online]. Available: http://ismi.sematech.org/modeling/simulation/index.htm#models

[27] G. A. Shafer, *Mathematical Theory of Evidence*. Princeton, NJ: Princeton Univ. Press, 1990.

[28] SIA press release. (2009). *Global Semiconductor Sales Fell by 2.8 Percent in 2008* [Online]. Available: http://www.sia-online.org/cs/papers_publications/press_release_detail?pressrelease.id=1534

[29] A. Stuart and J. K. Ord, *Kendall's Advanced Theory of Statistics*, 5th ed., vol. 1. New York: Oxford Univ. Press, 1987.

[30] P. Walley, *Statistical Reasoning with Imprecise Probabilities*. London, U.K.: Chapman and Hall, 1991.

[31] Y. Wang, "Imprecise probabilities with a generalized interval form," in *Proc. 3rd Int. Workshop REC*, 2008, pp. 45–59.

[32] Y. Wang, "Interpretable interval constraint solvers in semantic tolerance analysis," *Comput.-Aided Des. Applicat.*, vol. 5, no. 5, pp. 654–666, 2008.

[33] Y. Wang, "Imprecise probabilities based on generalized intervalsfor system reliability assessment," *Int. Journal of Reliability & Safety*, vol. 4 no. 4, pp. 319–342, 2010.

[34] K. Weichselberger, "The theory of interval-probability as a unifying concept for uncertainty," *Int. J. Approx. Reasoning*, vol. 24, nos. 2–3, pp. 149–170, 2000.

[35] G. Xiang, S. A Starks, V. Kreinovich, and L. Longpre, "Computing population variance and entropy under interval uncertainty: Linear-time algorithms," *Reliable Computing*, vol. 13, no. 6, pp. 467–488, 2007.

[36] F. Zouaoui and J. R. Wilson, "Accounting for input model and parameter uncertainty in simulation," in *Proc. Winter Simulation Conf.*, 2001.

[37] F. Zouaoui and J. R. Wilson, "Accounting for parameter uncertainty in simulation input modeling," in *Proc. Winter Simulation Conf.*, 2001.

Ola G. Batarseh (M'08) received the B.S. degree in industrial engineering from the University of Amman, Jordan, in 2006, and the M.S. and Ph.D. degrees in industrial engineering from University of Central Florida, Orlando, in 2008 and 2010, respectively.

Her current research interests include reliable modeling and simulation to support robust decision-making.

Dr. Batarseh is a member of the Institute for Operations Research and the Management Sciences, MD, and the Institute of Industrial Engineers, GA.

Dima Nazzal received the B.S. degree in industrial engineering from the University of Amman, Jordan, in 1998, and the M.S. degree in industrial engineering and management systems from the University of Central Florida, Orlando, in 2001, and the Ph.D. degree in industrial and systems engineering from the H. Milton Stewart School of Industrial and Systems Engineering, Georgia Institute of Technology, Atlanta, in 2006.

She is an Assistant Professor with the Department of Industrial Engineering and Management Systems, University of Central Florida. Her current research interests include analytical modeling of manufacturing and logistics systems.

Dr. Nazzal is a member of the Institute for Operations Research and the Management Sciences, MD, and the Institute of Industrial Engineers, GA.

Yan Wang (M'07) received the B.S. degree in electrical engineering from the Tsinghua University, Beijing, China, in 1996, the M.S. degree in electrical engineering from the Chinese Academy of Sciences, Beijing, China, in 1998, and the Ph.D. degree in industrial engineering from the University of Pittsburgh, Pittsburgh, PA, in 2003.

He is an Assistant Professor with the Woodruff School of Mechanical Engineering, Georgia Institute of Technology, Atlanta. His current research interests include engineering design, modeling and simulation, and uncertainty quantification.

Dr. Wang is a recipient of the NSF Career Awards and two Best Paper Awards. He has over 60 publications.